MedCrave
Step into the World of Research
International Journal of Biosensors & Bioelectronics

Research Article
Open Access
CrossMark

A experimental method to the study of wireless passive LC sensors

Abstract

This paper presents experiments related to the study of the operation of wireless passive LC resonant sensors that have important applications as the real-time implantable pressure sensor for monitoring of hypertension, pressure monitoring in eyes and in blood vessel. The presented experiments consisted of measurements of impedances, seen in an external module for different frequency values, to each capacitor used emulating a capacitive sensor placed in a blood vessel. The experimental results presented an excellent agreement with the analytical results and thus open the perspective of future studies as computational simulations perform and advanced experiments using capacitive sensors working along with better dimensioned coils.

Keywords: capacitive sensor, blood pressure, wireless measurements, resonant circuits

Volume 4 Issue 4 - 2018

Roberto Jacobe Rodrigues, Renan Melo De Freitas
Federal University of ABC, Brazil

Correspondence: Roberto Jacobe Rodrigues, Federal University of ABC, Avenida dos Estados, 5001-Bairro Santa Terezinha-Santo André-CEP 09210-580, Brazil, Tel +55-11-4996-0001, Email roberto.rodrigues@ufabc.edu.br

Received: June 25, 2018 | **Published:** July 11, 2018

Introduction

The wireless passive resonant LC sensors studies and developments have had a significant growing in the last two decades because these sensors do not need for power supply, wiring connections and electronics circuits.[1,2] These sensors represent great possibilities for monitoring of physiological parameters inside the human body.[3] An implantable device has to operate under harsh environment as a blood vessel.[2,3] Both development of an implantable intraocular pressure sensor for detection of glaucoma,[1] and blood pressure sensor for monitoring blood vessel pressure are application examples.[3–6] The measuring, i.e. pressure in most cases, changes the capacitance of the LC circuit placed within the environment being monitored (Figure 1). Thus the LC resonant frequency is changed as a pressure function. This resonant frequency is detected by a coil, magnetically coupled and outside the sensor environment. A readout circuit is connected to this external coil.[6] The coil L_1 receives an AC signal from Signal Generator, which induces an electrical current in the coil L_2 (Lei de Faraday-Lenz). The energy changes between L_2 and the capacitor C induces an electrical current in the coil L_1, which will be detected as coupled impedance, measured between (a) and (b) points marked in the Figure 1. The total impedance measured between (a) and (b) points is given by Equation 1.[2,7]

$$\dot{Z}_i = R_1 + j\omega L_1 + \frac{(\omega M)^2}{R_2 + j\omega L_2 - j\left(\frac{1}{\omega C}\right)} \quad (1)$$

where ω is the angular frequency (rad/s), L_1 and L_2 are coils inductances (Henry), R_1 and R_2 are coils series resistors (Ohm), C will work as if it were the measuring dependent capacitance (Faraday) and M is the Mutual inductance (Henry).Therefore, this work presents an experimental method to confirm the impedance dependency, $\dot{Z}_l$ (module and phase) with different capacitance values, C. In the future experiments, the capacitor will be replaced by a capacitive sensor and the coils will be designed to perform the best performance.

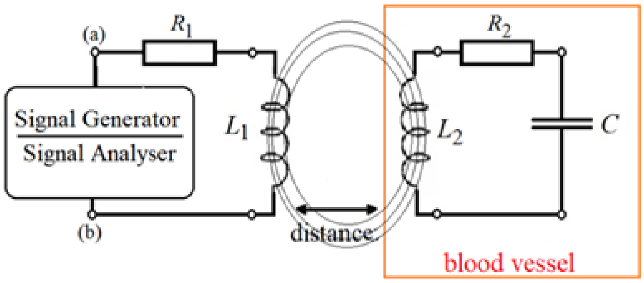

Figure 1 Wireless passive LC sensor.

Materials and methods

The Mutual inductance was determined by using the circuit showed in Figure 2. The nominal inductances values L_1 e L_2 are 22mH and the measured ones, by LCR Minipa MX-1010 equipment, were 21,38mH, equals for both coils. The adopted resistor was R = 1kΩ. The Mutual inductance value is given by:[7]

$$\dot{V}_2 = j\omega M\dot{I} \quad (2)$$

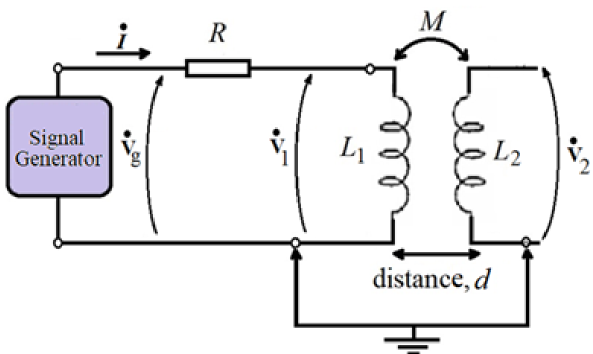

Figure 2 Mutual inductance determination.

The electrical current, $\dot{I}$ is the Ohm's Law application of the difference of the measured signals read out from Oscilloscope $(\dot{V}_g - \dot{V}_1)$ on *R*. The graph of the Mutual inductance vs coils distances is shown in Figure 3. The circuit, for experimental determination of the dependence between impedance (Module and Phase) and resonant frequency, is shown in Figure 4.

The circuit presented in Figure 4 is the same one presented in Figure 2, but adding R_2=47Ω resistor and capacitor. The adopted capacitor nominal values were 10nF, 33nF and 68nF. The distance in between coils was $10x10^{-3}$m. Thus the Mutual inductance will be M ≈ 2,2mH (Figure 3). For each adopted capacitance value, two curves were drawn: the impedance module vs frequency and the impedance phase vs frequency. These graphs were compared with analytical results from Equation 1. A 2V peak-to-peak sinusoidal signal was adjusted on signal generator. The impedance modules values were obtained from V_g/I_{R1} ratio, where I_{R1} is the V_{R1}/R_1 ratio (Figure 4). Already the impedance phase φ (degree) is the phase difference measured between signals V_g and V_{R1} (Figure 6).

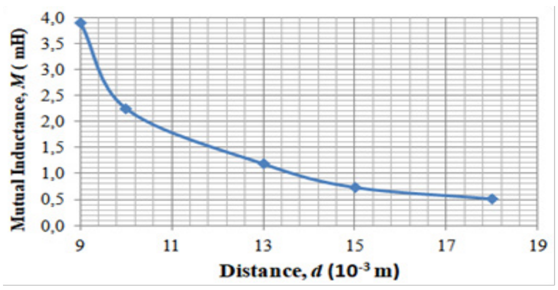

Figure 3 Mutual inductance vs coils distances.

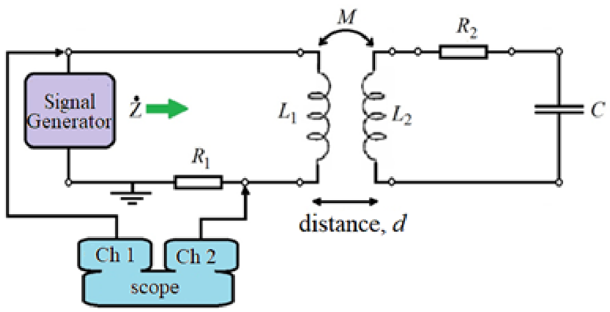

Figure 4 Circuit to measurement of the impedance dependence with the applied signal frequency and the capacitors.

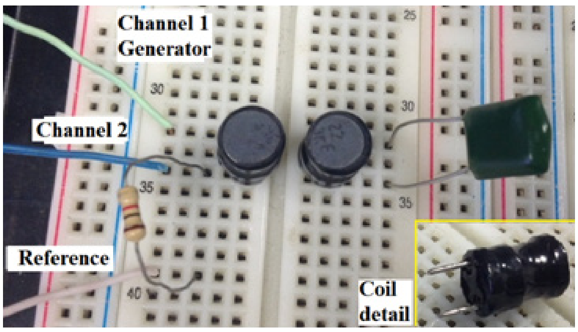

Figure 5 Assembled circuit picture and a detail of the coil type used in tests.

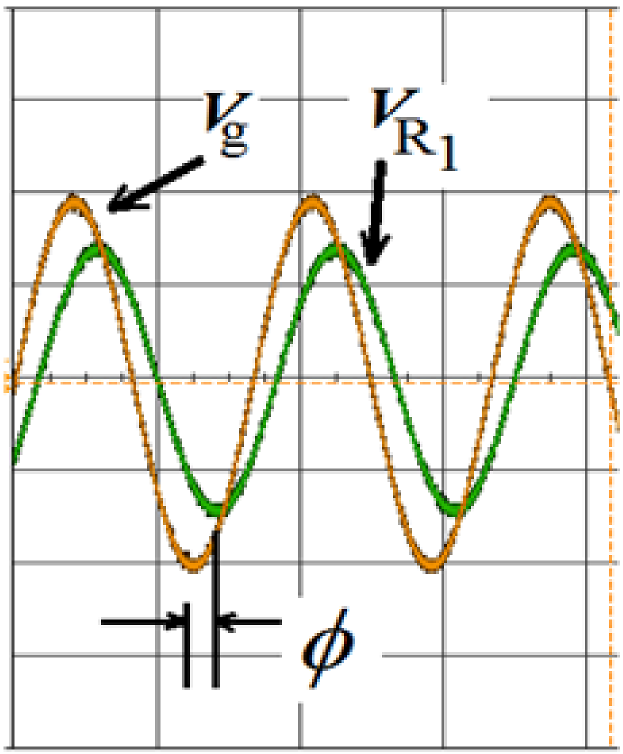

Figure 6 Relation between signals as measured on oscilloscope to C = 33nF.

Results

The Figure 7 shows a excellent agreement between analytical and experimental to a 10nF capacitor. This agreement also occurred to 33nF and 68nF ones. Moreover, it was obtained a good qualitatively agreement with literature results.[4,6] The resonant frequency values were determined in agreement with literature procedures,[6] and showed arrowed on (Figure 7) (Figure 8). The resonant frequency value is given by Equation 3:[4]

$$f_o = \frac{1}{2\pi\sqrt{L_2 C}} \quad (3)$$

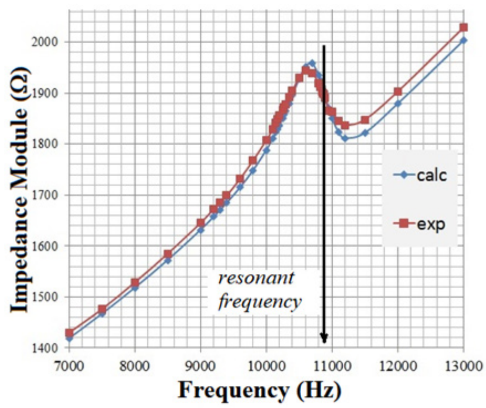

Figure 7 Impedance x Frequency to C = 10nF.

Citation: Rodrigues RJ, Freitas RM. A experimental method to the study of wireless passive LC sensors. *Int J Biosen Bioelectron.* 2018;4(4):175–177.
DOI: 10.15406/ijbsbe.2018.04.00121

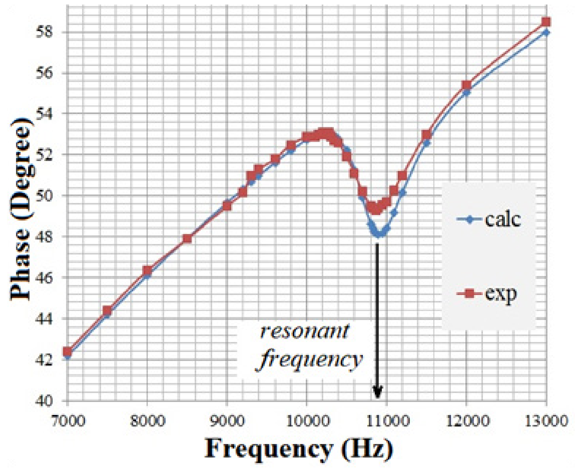

Figure 8 Phase vs Frequency to C = 10nF.

The resonant frequency is the frequency where the phase begin increase again.[4,6] The resonant frequencies obtained were around 4kHz from 68nF capacitor, around 6kHz from 33nF and around 11kHz from 10nF.

The behavior of the spectrum with the resonant frequencies to each capacitor is shown by (Figure 9) (Figure 10), having respectively the impedance module and phase.

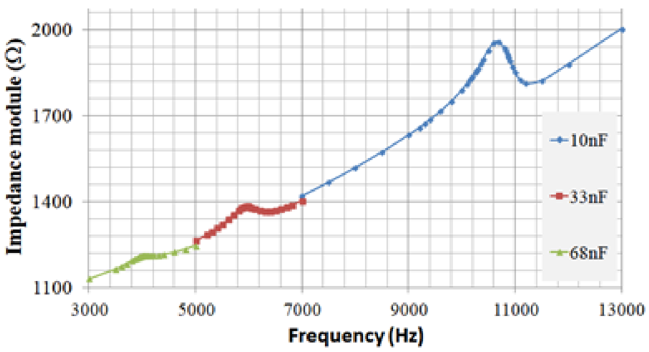

Figure 9 Impedance module vs frequency and adopted capacitors.

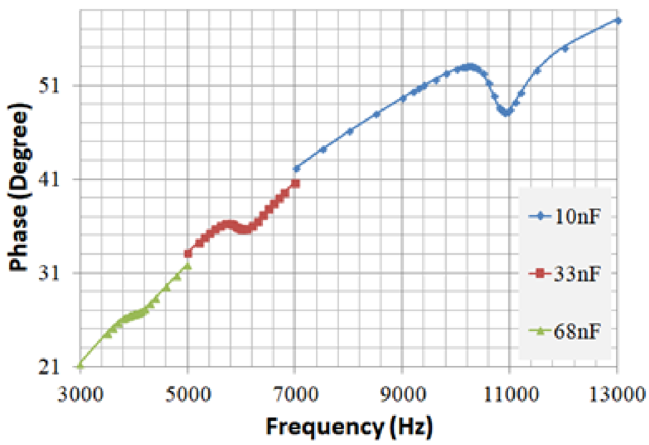

Figure 10 Phase vs Frequency and adopted capacitors.

Discussion

The resonant frequency, pointed by arrows, from (Figure 7) (Figure 8) agree with literature procedure.[4,6] The (Figure 9) (Figure 10) show that capacitance values below 10nF results a lower amplitude variation around resonant frequency. Therefore, new tests should be performed with lowers inductances values, µH rather than mH, as well as lower capacitances. Thus, the frequencies quite superior to adopted frequencies in this presented experiment, for example the frequencies presented in literature.[2,8] In addition, longer distances will be tested.

Due to influence both coupling coefficient and quality factor, the calculated value of the resonant frequency, by Equation 3, do not agree with one obtained graphically by (Figure 7) (Figure 8).[4] Thus, in future works, studies should be performed to analyze the influence of the quality factor on the performance of the system as well as on the experimental frequency. More precise procedures for the determination of the resonance frequency should be studied.

Conclusion

An experimental procedure using components available in the didactic laboratory was proposed for the study of a system similar to that used in applications such as the monitoring of blood pressure in real time from a blood vessel.[3] The experimental results indicated a agreement with the analytical results obtained and thus open the perspective to new studies and new experiments, but using, instead of fixed capacitors, capacitive sensors immersed in environments being monitored, as well as with the use of better dimensioned coils. The purpose of this article was reached because it has been shown that a resonant LC circuit with variable capacitance values can communicate wirelessly with a distant coil.

Acknowledgements

The author would like to acknowledge Federal University of ABC (UFABC) for provided facilities and equipments.

Conflict of interest

Author declares that there is no conflict of interest.

References

1. Collins C. Miniature passive pressure transensor for implanting in the eye. *IEEE Transactions on bio-medical engineering*. 1967;14(2):74–83.
2. Wang Y, Yi Jia, Qiushui Chen, et al. A passive wireless temperature sensor for harsh environment applications. *Sensors*. 2008;8:7982–7995.
3. Clausen I, Glott T. Development of Clinically Relevant Implantable Pressure Sensors: Perspectives and Challenges. *Sensors*. 2014;14:17686–17702.
4. Li C, Tan Q, Jia P, et al. Review of Research status and development trends of wireless passive LC resonant sensors for harsh environments. *Sensors*. 2015;15:13097–13109.
5. Zhai J, How TV, Hon B Design and modelling of a passive wireless pressure sensor. *CIRP Ann Manuf Technol*. 2010;59:187–190.
6. Nopper R, Remigius Niekrawietz, Leonhard Reindl, et al. Wireless readout of passive LC sensors. *IEEE Trans Instrum Meas*. 2010;59:2450–2457.
7. Miller WC, Robbins AH. Análise De Circuitos, Teoria e Prática. *Cengage Learning*. 2010:2.
8. Fonseca MA, English JM, Allen MG, et al. Wireless micromachined ceramic pressure sensor for high-temperature applications. *J Microelectromechan Syst*. 2002;11:337–343.

Citation: Rodrigues RJ, Freitas RM. A experimental method to the study of wireless passive LC sensors. *Int J Biosen Bioelectron.* 2018;4(4):175–177.
DOI: 10.15406/ijbsbe.2018.04.00121